

# OPTIMAL DESIGN SELECTION AND ANALYSIS OF SINGLE SIDED LINEAR INDUCTION MOTOR

**Dr. Srinivasan Arumugam<sup>1</sup>, Sivakumar Arunachalam<sup>2</sup> and Dr. Vijayan Velappan<sup>3</sup>**

<sup>1</sup>Associate professor, Department of Mechatronics, Chennai Institute of Technology, Chennai-69, India.

<sup>2</sup>Associate professor, Department of EEE, Panimalar Engineering College, Chennai-123, India.

<sup>3</sup>professor, Department of EIE, St. Joseph's College of Engineering, Chennai-600119

<sup>1</sup>a.srinivasan2025@gmail.com, <sup>2</sup>arunsiva75@gmail.com and <sup>3</sup>vinvpn@gmail.com

**Abstract**-Linear induction machines (LIMs) are largely utilized recently for speedier transport usage and such motors attain thrust openly with no gear apparatus for coupling operation system. Additionally LIMs bear several other advantages namely with no complex structure and simple repairing. LIMs bear great demerits: moderate efficiency and poor power factor. Such demerits produce huge loss on energy and an increase the amount of input current and thereby high transmission grid power. This paper uses a multi-objective GA optimization technique conjoined cuckoo optimization algorithm (COA) to improve direct application parameters like efficiency thrust, power factor and input current is established, simultaneously. The proposed intelligent mechanism is introduced on potential of biological-dependent optimization algorithms in choosing for the optimal design variables. Here, SSLIM system is used to depict the performance of the design procedure and optimization. The salient characteristics of the GA, COA and GA-COA are because of their potentiality to simultaneously edify a local search, when exploring globally values in search space. Additionally, MATLAB simulation produces to illustrate that suggested algorithms bear less correlation on variables variations. The used optimization technique too was quite rapid, need less duration to compute for optimal design variables in search space.

## 1. INTRODUCTION

Motor has been significantly widely used to reduce any kind of mechanical efforts, which directs to use in the transporting or load carrying mechanisms. A particular kind of induction motor called linear induction motor (LIM) is utilized for the performance of linear motion namely railway transport, escalator, automatic unmanned vehicles, liquid pumping and so on. Linear Induction motor is a type of rotary squirrel cage induction motor, break along its axis of rotation radially and curves out that forms direct linear induction motor (refer Figure 1), in other words, it is unrolled or flattened rotary induction motor. The concept behind linear

electric motor is similar to that of customary classical rotary type induction motor (RIM). Recently, LIM design came to an existence for enhancing the efficiency of a linear system in which the concept of traditional rotary motor along with rotary to linear converters is used. LIM is dissociative and excessive speed motor, Linear motor works on the same fundamental like rotary, squirrel induction motor. 1800 inches/sec [45 m/s] is the maximum achievable speed in LIM. LIM can be used in applications when precise positioning is not needed.

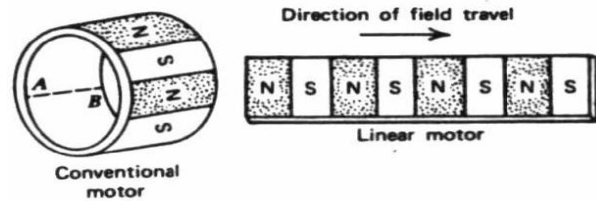


Figure 1 (a)

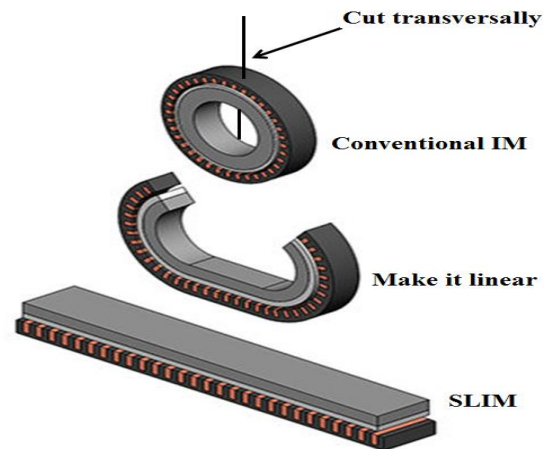


Figure 1 (b)

Figure 1 (a) comparison of rotary conventional motor and linear induction motor (b) illustration of converting conventional rotary motor to single lined linear induction motor,

## 2. DESIGN OF LIM

LIM are categorized into two types: single-sided LIM and double sided LIM by its structure. The stator primary length is just placed over the secondary in case of single-sided LIM (SSLIM), alternatively it contains the primary with lamination, and a secondary with numerous lot of aluminum conductor sheets bearing the back with iron as its return path interior of magnetic flux whereas in double-sided LIM (DSLIM), the stator primary is placed on both sides of secondary (Refer Figure 2), alternatively it comprises of two stacks of primary with laminations, and a secondary of an aluminum in the center. This arrangement is further categorized as short primary and long primary, for the applications of transportation a long secondary is desired. They are too categorized in other way as high-speed and low-speed LIMs. There is another type based on its construction as Tubular LIM (TLIM) where the primary and secondary are positioned co-axially.

The SSLIM considers basic, with reduced mechanical loss, superior acceleration furthermore deceleration on comparing with previously fashioned rotary motors. Due to large air gap length, SSLIM is largely prone by its lower efficiency which is drastic on lesser load in particular. Additionally, split open kind of magnetic circuit and disparity on the width of primary and secondary leads to set off the specific experiences namely the edge effect on transverse and end effect on longitude. These phenomena might reduce its magnetizing inductance and enhance its resistance of secondary, and thereby, its efficiency will be declining moreover [1].

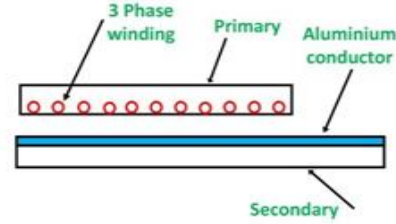


Figure 2(a) Structure of SSLIM

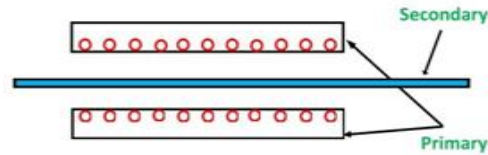


Figure 2 (b) Structure of DSLIM

## 3. SSLIM OPERATION

The traditional 3 phase rotary induction motor comprises two main, fundamental elements: the stator and rotor. The stator comprises a balanced poly-phase winding that placed evenly in the slots of the stator by its perimeter. The stator generates a magnetic field of sinusoid distribution in the air-gap which it rotates at the uniform speed  $2\omega/P$ , where  $\omega$  denotes the supply exciting frequency  $f$  by  $\omega = 2\pi f$  and  $P$  is the number of poles. The rotor voltage is induced because of the comparative movement between the conductors of the rotor and the magnetic field. Such induction of voltage will produce a current which this flows in the rotor and in turn produce a magnetic field. The two magnetic fields on interaction will generate a torque which pulls the rotor in field direction. This concept will not be changed when a continuous sheet of conducting material is placed instead of the squirrel cage.

The study between the rotary induction motor and the SSLIM usually relies on the open air gap which becomes the fundamental difference between them. The edge and end effects devalue the performance and put SSLIM under doubt the ground reality of the applications of SSLIMs [2]. The LIM air gaps are normally with greater magnitude comparing conventional induction motors. Electromagnetic vibration and noise are chiefly produced due to electromagnetic forces generating out of composite of harmonic fluxes in air-gap [3]

#### 4. SLIM EQUATIONS

**Slip:** Induction motors usually run up to the speed of  $V_r$  which is little less comparing synchronous velocity  $V_s$ . Slip defines the variation between the speed of stator magnetic field rotation and the speed of the rotor. Slip is the comparative movement between the field and rotor conductors required in the induction motor to generate a voltage in the rotor and it is stated as

$$S = \frac{V_s - V_r}{V_s} \quad (1)$$

The synchronous velocity  $V_s$  of SSLIM is the identical to that of RIM, stated as

$$V_s = \frac{2\omega R}{p} = 2f\tau \quad (2)$$

In which,  $R$  is the radius of the stator of the RIM. The linear speed will not rely upon the number of poles however on  $p$  the pitch of the pole. The  $\tau$  is the distance between adjacent poles on the stator circumference termed the pitch of the pole pitch described by

$$\tau = \frac{2\pi R}{p} \quad (3)$$

Being the circumference of the stator of the RIM,  $2\pi R$ , stated by (3) is same to the length of the stator of SSLIM,  $L_s$ . Hence, pitch of the pole of SLIM is

$$\tau = \frac{L_s}{p} \quad (4)$$

The air-gap as depicted in Figure 3 is the clearance between the rotor outer and the stator of the SLIM.

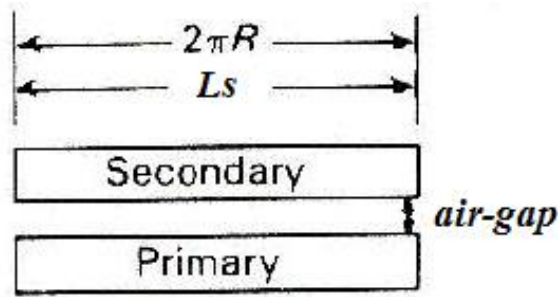


Figure 3 the clearance between the stator and the rotor as air-gap

**Stator Current density:** The stator contains several coils, and each coil does have several turns

of wires as windings lodged in the slots of laminated iron. The current that flows in the windings is considered imaginatively as current distributed on infinitely thin layer over the stator surface lining the air gap. Such current is termed as current sheet. This current sheet generates the sinusoidal magneto-motive force in the air gap identically generated by the conductors. The current sheet density ( $J_m$ ) is calculated from

$$J_m = \frac{2\sqrt{2}mK_w N_c I_1}{L_s} \quad (5)$$

In which  $k_w$  is called winding factor,  $m$  is the number of supply phases to the motor,  $N_c$  is the number of turns per stator slot,  $I_1$  is the RMS input current and  $L_s$  is the stator length. The  $k_w$  can be described by multiplying the pitch factor  $k_p$  and distribution factor  $k_d$

$$K_w = K_p K_d \quad (6)$$

$$K_p = \sin\left(\frac{\theta_p}{2}\right) \quad K_d = \frac{\sin\left(\frac{q_1 \alpha}{2}\right)}{q_1 \sin\left(\frac{\alpha}{2}\right)} \quad (7)$$

In which  $\theta_p$  is the coil span in electrical degrees,  $q_1$  is the number of slots per pole per phase and  $\alpha$  is the slot angle stated as

$$\alpha = \frac{\pi}{mq_1} \quad (8)$$

**Input power:** The input power of the stator windings is described

$$P_1 = mV_1 I_1 \cos\phi \quad (9)$$

In which  $m$  is the number of supply phases,  $V_1$  and  $I_1$  are the input RMS voltage and current of the phase, respectively, and the  $\cos\phi$  power factor in which  $\phi$  is the phase difference between  $V_1$  and  $I_1$ . The component of the stator copper losses due to windings and the component of stator core and teeth iron losses are comprised in the input power. The rest of the input power is carried to the rotor via the magnetic field present in the air-gap. The power carried to the rotor is deduced as the mechanical power generated by the rotor by

ignoring the losses due to rotor conductor and friction. The complete output mechanical power generated by the rotor can be stated as

$$P_o = F_s V_r \quad (10)$$

In which  $F_s$  is the thrust produced on the rotor because of the stator electromagnetic flux and  $V_r$  is the rotor speed.

**Efficiency:** The efficiency  $\eta$  of SLIM is evaluated using

$$\eta = \frac{P_o}{P_i} = \frac{F_s V_r}{m V_1 I_1 \cos \phi} \quad (11)$$

Hence the rated input phase current can be calculated using

$$I_1 = \frac{F_s V_r}{m V_1 \eta \cos \phi} \quad (12)$$

**Induced voltage:** A stator coil with  $N$  turns bearing a current  $I$  amperes and  $\Phi$  be the consequent flux developed by coupling with the coil. Assume air-gap flux density  $\Phi$  is simply a sinusoid; subsequently it will be described

$$\Phi = \Phi_p \sin \omega t \quad (13)$$

In which  $\Phi_p$  is defined as a magnitude of the flux linkage per pole  $\Phi$ . The induced voltage per turn in the stator coil because of changing flux can be stated by applying single derivative in the equation (13) and is depicted

$$e = \frac{d\Phi}{dt} = \omega \Phi_p \cos \omega t \quad (14)$$

With its RMS value  $E_1$

$$E_1 = \frac{2\pi}{\sqrt{2}} f \Phi_p = \sqrt{2} \pi f \Phi_p \quad (15)$$

If the stator coil has  $NI$  turns per phase with winding factor  $k_w$ , then (15) changed into

$$E_1 = \sqrt{2} \pi f \Phi_p K_w N_1$$

## Geometry of the SSLIM

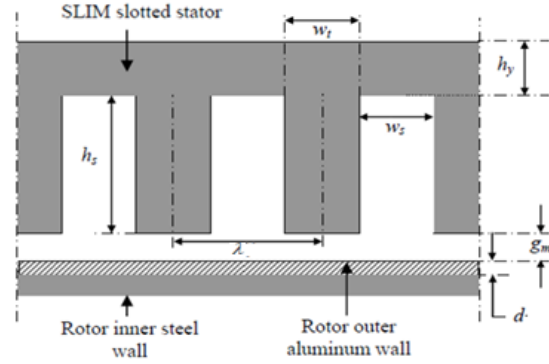


Figure 4 SSLIM dimensions

The air-gap is so significant parameter of a machine. The  $g_e$  effective air-gap of the SLIM is non-identical to the physical air-gap,  $g_m$ , due to the stator slotted construction, as depicted in Fig 4 [4].

$$g_e = K_c g_o \quad g_o = g_m + d \quad (16)$$

Where  $g_o$  is the magnetic air gap,  $d$  is rotor surface conducting layer thickness and  $k_c$  is carter's coefficient

$$K_c = \frac{\lambda}{\lambda - \gamma g_o} \quad (17)$$

Where  $\lambda$  is the slot pitch (Refer Figure 4), the distance between two adjacent stator slots and  $\gamma$  is a parameter defined by

$$\gamma = \frac{4}{\pi} \left[ \frac{w_s}{2g_o} \arctan \left( \frac{w_s}{2g_o} \right) - \ln \sqrt{1 + \left( \frac{w_s}{2g_o} \right)^2} \right] \quad (18)$$

Where  $w_s$  is the stator slot width. The sum of slot width and tooth width is termed as slot pitch and described as

$$w_s + w_t = \lambda \quad (19)$$

Where,  $w_t$  is the tooth width. From the Figure 4, the depth  $h_s$  of stator slot can be computed using

$$h_s = \frac{A_s}{w_s} \quad (20)$$

Where  $A_s$  is the area of stator cross section and it is calculated considering 30% is being packed in the stator slot with insulating material

$$A_s = \frac{10}{7} N_c A_w \quad (21)$$

Where  $A_w$  is the cross section of the conductor without insulation used in stator winding and  $N_c$

number of turns per stator slot can be obtained using

$$A_w = \frac{I_1}{J_1} \quad N_c = \frac{N_1}{pq_1} \quad (22)$$

In which,  $I_1$  and  $J_1$  are the rated input phase current and stator current density described earlier. The main force concerned with the LIM is the thrust. The LIM generates a thrust which depends on the square of the applied voltage, and hence this decreases when the slip gets decreased comparably with an induction motor of greater rotor resistance.

#### Equivalent circuit of SSLIM

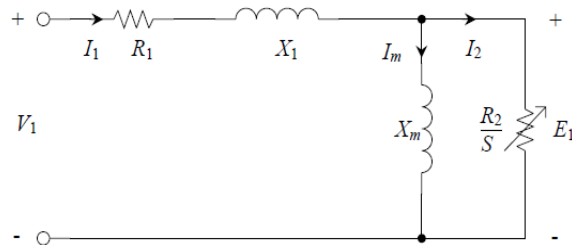


Figure 5 Stator equivalent circuits per phase for the SSLIM

SSLIM corresponding approximate circuit per phase is depicted in Figure 5. The losses due to core are ignored due to practical air-gap flux density directs to lessen flux densities in the core and thus otherwiseless core losses. Skin effect is too less at particular frequency for a SLIM with a slender conductive sheet on the secondary surface. Hence, the equivalent circuit for rotor inductance is insignificant [5]. The rest significant parameters are depicted in Figure 5 and are described

#### Stator resistance $R_1$ per phase

$R_1$  is evaluated using

$$R_1 = \rho_w \frac{l_w}{A_w} \quad (23)$$

In which,  $\rho_w$  is the volume resistivity,  $l_w$  is the length and  $A_w$  is the cross-sectional area of the copper conductor utilized in the stator winding per phase. The length  $l_w$  is evaluated using

$$l_w = N_1 l_{w1}; l_{w1} = 2(W_s + l_{ce}); l_{ce} = \frac{\theta_p}{180^\circ} \tau \quad (24)$$

Where  $W_s$  is the stator width,  $l_{w1}$  is the average length of one turn of stator coil and  $l_{ce}$  is the length of connecting end of the stator coil

#### Stator-slot leakage reactance $X_1$ per phase

The flux that generated in the stator coils is not entirely coupled to the rotor conductors; hence there exists certain leakage flux in the slots of the stator slots and thus stator-slot leakage reactance  $X_1$ . Such leakage flux is produced separately by a coil within a stator slot and resulted due to the stator iron core slot openings. The stator of SSLIM bearing open rectangular slots with a double-layer winding,  $X_1$  is determined [6]

$$X_1 = \frac{2\mu_o \pi f \left[ \left( \lambda_s \left( 1 + \frac{3}{p} \right) + \lambda_d \right) \frac{W_s}{q_1} + \lambda_e l_{ce} \right] N_1^2}{p} \quad (25)$$

where

$$\lambda_s = \frac{h_s (1 + 3K_p)}{12w_s} \quad \lambda_e = 0.3(3K_p - 1)$$

$$\lambda_d = \frac{5 \left( \frac{g_e}{w_s} \right)}{5 + 4 \left( \frac{g_o}{w_s} \right)} \quad (26)$$

#### Magnetizing reactance $X_m$ per phase

From Figure 5, the magnetizing reactance  $X_m$  per phase can be determined

$$X_m = \frac{24\mu_o \pi f W_{se} K_w N_1^2 \tau}{\pi^2 p g_e} \quad (27)$$

Where  $\mu_o$  is permeability of free space and  $W_{se}$  is the equivalent stator width described

$$W_{se} = W_s + g_o \quad (28)$$

#### Rotor resistance $R_2$ per-phase

The rotor resistance per-phase  $R_2$  is dependent on slip.  $R_2$  is evaluated using the goodness factor  $G$  and the magnetizing reactance per-phase  $X_m$

$$R_2 = \frac{X_m}{G} \quad (29)$$

Where, the goodness factor  $G$  is described [1]

$$G = \frac{2\mu_o f \tau^2}{\pi \left( \frac{\rho_r}{d} \right) g_e} \quad (30)$$

Where,  $\rho_r$  is the volume resistivity of the rotor surface conductor that is aluminum.

#### Rotor current

The magnitude of the rotor phase current  $I_2$  is observed

$$I_2 = \frac{X_m}{\sqrt{\left( \frac{R_2}{s} \right)^2 + X_m^2}} I_1 \quad (31)$$

On replacing the  $R_2$  using (29), the rotor phase current  $I_2$  becomes

$$I_2 = \frac{I_1}{\sqrt{S^2 G^2 + 1}} \quad (32)$$

#### Thrust and efficiency

The stator input power is used in generating effective mechanical power that is applied on the rotor and to justify the losses of the rotor copper. In terms of the equivalent circuit components, the mechanical power generated by the rotor is the power carried across the air-gap from the stator to the rotor  $mI_2^2 R_2 / S$  subtracted with  $mI_2^2 R_2$  [29]

$$P_o = mI_2^2 \frac{R_2}{S} - mI_2^2 R_2 = mI_2^2 R_2 \left( \frac{1-S}{S} \right) \quad (33)$$

Substituting the equation (10) for  $P_o$  and equation (1) for  $V_r = V_s(1-S)$  in (33), the electromagnetic thrust produced in the stator of SSLIM is

$$F_s = \frac{mI_2^2 R_2}{V_s S} \quad (34)$$

It is the quite usual way to describe electromagnetic thrust for a SSLIM ascertained using the rotor phase current  $I_2$ . But, regarding SSLIM equivalent circuit depicted in Figure 5, in which the core losses are ignored,  $F_s$  can be stated using stator phase current  $I_1$ . Substituting equation (32) in equation (34), the SSLIM thrust turns [28]

$$F_s = \frac{mI_1^2 R_2}{\left[ \frac{1}{(SG)^2} + 1 \right] V_s S} \quad (35)$$

The SSLIM input active power is the summation of the output power and the copper losses from the stator and rotor

$$P_i = P_o + mI_1^2 R_1 + mI_2^2 R_2 \quad (36)$$

Where,  $mI_1^2 R_1$  is the stator copper loss. On replacing equations (33), and (35) in (36) produces

$$P_i = F_s V_s + mI_1^2 R_1 \quad (37)$$

The SSLIM efficiency is determined by evaluating the ratio of (33) and (37), such a way

$$\eta = \frac{P_o}{P_i} \quad (38)$$

#### Analysis of End effect

A new flux is persistently generated at the ingress of the primary yoke being the primary moves, when prevailing flux vanishes at the egress. Unforeseen production and extinction of the pervading field invokes eddy currents on secondary layer. The end effects cannot be observable in RIM. In case of LIMs, end effects turn progressively applicable with the rise in the relative velocity between primary and secondary. Hence, the end effects must be studied in terms of velocity. The eddy current at the ingress increases quite speedily to reflect the magnetizing current, neutralizing the air-gap flux at the ingress whereas the eddy current at the egress produces a type of weak field, pulling the primary core movement.

$$Q = \frac{L_s R_2}{(L_m + L_2) V_r} \quad (39)$$

Where,  $Q$  is the normalized motor length

The thrust, efficiency and power factor are evaluated from

$$F_s = \frac{3I_2^2 R_2}{S 2\mathcal{F}_1 \left[ \left( \frac{1}{SG_{ei}} \right)^2 + 1 \right]} \quad (40)$$

$$\eta = \frac{F_s 2\mathcal{F}_1 (1-S)}{F_1 2\mathcal{F}_1 + 3R_1 I_1^2} \quad (41)$$



$$\cos \phi = \frac{F_s 2\mathcal{F}_1 + 3R_1 I_1^2}{3V_1 I_1} \quad (42)$$

By using the following set of equations

$$G_{ei} = \frac{2\mu_o f \tau^2 \sigma_{ei} d_2}{\pi g_{ei}}$$

$$g_{ei} = \frac{K_i K_c (1 + K_p) g_o}{K_m}$$

$$\sigma_e = \sigma_{2e} + \sigma_{1e} \frac{\sigma_i}{d_2}$$

$$g_e = g K_e (1 + K_s)$$

$$\sigma_{1e} = \frac{\sigma_1}{K_{fc}} \quad \sigma_{2e} = \sigma_i K_t$$

$$K_{fc} = \left(1 - \frac{tgh(\beta a_e)}{\beta a_e}\right)^{-1}$$

$$K_t = 1 - \frac{tgh(0.5\beta h)}{0.5\beta h [1 + tgh(0.5\beta h) tgh(\beta C)]}$$

$$C = 0.5(h_2 - h) a_e = h + g_o \quad g_o = g + d_2$$

$$K_s = \frac{\mu_1}{\mu_o \delta_i g_o K_c \beta^2}$$

$$\delta_i = \text{Re} \left[ \frac{1}{(\beta^2 + j\omega\mu_1 S \sigma_{1e})^{0.5}} \right]$$

$\sigma_{1e}$  and  $\sigma_{2e}$  are equivalent back iron conductivity and Equivalent conducting plate conductivity respectively.  $K_s$ ,  $K_c$ ,  $K_{fe}$ ,  $K_t$  are saturation factor, Carter coefficient, Edge factor due to back iron and Edge factor due to conducting plate respectively.  $h$  and  $h_2$  are effective primary width and secondary width,  $\delta_i$  is the depth of field penetration in iron,  $\mu_1$  is permeability of back iron and  $\beta = \pi/\tau$ .

## 5. CUCKOO OPTIMIZATION ALGORITHM

The Algorithm of cuckoo optimization algorithm is a kind of optimization algorithm [7]. With the motivation by the constrained brooding parasitism in certain species of cuckoo by laying their eggs in the other host birds', belong different species, nests, this algorithm was developed. Certain host birds will busily involve in open dispute with the encroaching cuckoos. When a host bird finds the eggs do not belong to it, it will either push away these strange eggs or just disown

its nest. Certain species of cuckoo namely the brood parasite *Tapera* acquired character like so that female parasite cuckoos are regularly quite distinguished in imitating egg colors and pattern of a certain selected host species. Cuckoo search optimization with such breeding behavior hence can be used for several optimization challenges. It appears that it will dominate other meta-heuristic algorithms for operations. Cuckoo search (CS) utilizes the illustrations as depicted in Figure 7:

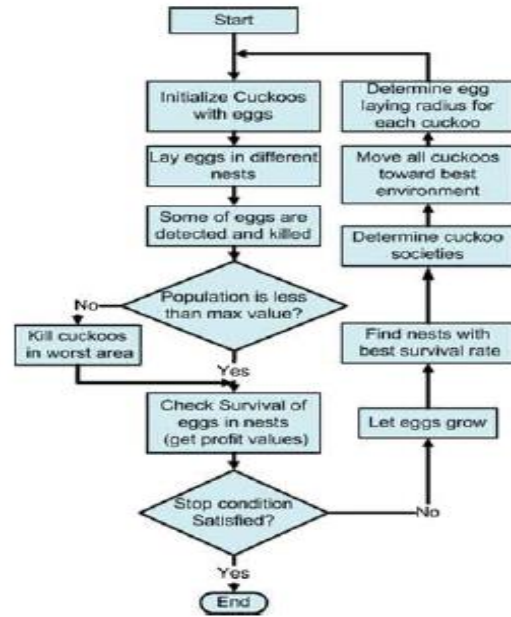


Figure 7 Flowchart for cuckoo search

### Algorithm of cuckoo search

1. Begin bird territory with certain probable points on the profit function
2. Devote certain eggs to each bird
3. Detail the egg laying radius (ELR) for each bird
4. Assume birds to lay eggs within their associated ELR
5. Ruin those eggs found by host bird
6. Assume eggs hatch and chicks grow
7. Evaluate the territory of each newly grown bird
8. Restrict maximum number of cuckoo in territory and destroy those who dwell in worst home
9. Group the birds and determine best family and determine target home
10. Assume new cuckoo population migrate toward target home
11. When halting criterion is achieved stop, else go to 2

Machine Parameters	Minimum value	Maximum value
Primary current density(A/m <sup>2</sup> )	829.115	1.4141e6
Primary width	1m	3.14m
Secondary sheet thickness (Aluminum)	1mm	10mm
Slip	0.1	0.5
Air gap length (mm)	10mm	50mm
Number of pole pairs	2	8
Tooth width to slot pitch ratio	0.0149/ 0.0574	0.035/0.05 74
Frequency (Hz)	50	250
Efficiency (%)	70	
Power factor	0.8	

## 6. GENETIC ALGORITHM (GA)

In common, optimization using GA is a stochastic search procedure which includes generating randomly viable design challenges and subsequently methodically computes and edifies the solutions till halting conditions or defined population size stopping is attained. Three basic operators included in this search operations: selection, crossover and mutation. The GA realization steps are depicted [9]

1. Initialize parameter and set the objective function
2. Produce first population at random
3. Estimate the population fitness using objective function
4. Test for convergence. When fulfilled then stop otherwise proceed.
5. Begin reproduction process by selection and perform the operators crossover, mutation
6. Results new generation. In order to proceed with the optimization, repeat from step 3.

## 7. PROPOSED METHOD

Numerous SSLIM variables and dimensions are selected as design variables whose values are determined in optimization procedure by GA and COA combination technique. In this paper, design variables are the primary winding current density, the primary width, the aluminum sheet thickness, air-gap length, number of pole pairs, tool width to slot pitch ratio and the maximum thrust

slip. Table 1 depicts the constraints on the design procedure. The rated thrust, the input voltage, supply frequency, supply phase and the mechanical speed the main fixed features the draft procedure are 8161 N, 440 V, 50 Hz, 3-phase and 15.5 m/s, respectively.

Table 1 Machine variables constraints for cuckoo optimization

## 7.1 GA OPTIMIZATION

This uses **gamultiobj** of the MATLAB by [d\_a, fval\_a]=gamultiobj(fitness,nvar); where d\_a is the thickness of aluminum with fitness function. The formulation of the objective function is the following:

$$F(x) = \begin{cases} F(x) - P(g_j(x), r) & \text{If } F(x) - P(g_j(x), r) > 0 \\ 0 & \text{If } F(x) - P(g_j(x), r) \leq 0 \end{cases}$$

Where, F(x) is the objective function with the thrust, current density, power factor, efficiency or torque, and additionally r is the cost value that is connected to the value of objective function. The cost function, P(g<sub>j</sub>(x),r), is described regarding of the kind of inequality applied. Through external cost function, the problems of constrained problems are changed to problems of unconstrained by rejecting constraints. Pertaining constraints, cost function is described;

$$P(g_j(x), r) = \begin{cases} r \sum [\max(0, g_j)]^2 & j = 1, \dots, 6 \\ r \sum [\min(0, g_j)]^2 & j = 7, 8 \end{cases}$$

## 7.2 COA OPTIMIZATION

To achieve an optimal draft considering both power factor and efficiency, the fitness function is described as  $J_r(x_1, x_2, \dots, x_n) = d_{al}(x_1, x_2, \dots, x_n)^k \eta(x_1, x_2, \dots, x_n)^{k_1} PF(x_1, x_2, \dots, x_n)^{k_2}$ . Here k, k<sub>1</sub> and k<sub>2</sub> are fixed numbers and are x<sub>1</sub>, x<sub>2</sub>, ..., x<sub>n</sub> are design variables [8].

COA Parameters	Max	Min
Optimized parameter	Array	
Cuckoo initial population	5	
Number of Eggs for every cuckoo	2	4
Number of clusters	1	



Number of cuckoo visit in territory at a time	10	5
otion coefficient	9	
Radius coefficient	5	
Cuckoo population variance	1e-13	

Table 2 Design variables constraints for cuckoo optimization

## 8 RESULTS

Table 3: Results of optimizations

Parameter $V_r=16.4, P=4, s=0.1$	Results
Efficiency (%)	88
Power factor	0.8
Output thrust (N)	$2.8 \times 10^4$ N

Table 4: GA-COA Results of optimizations with aluminum thickness

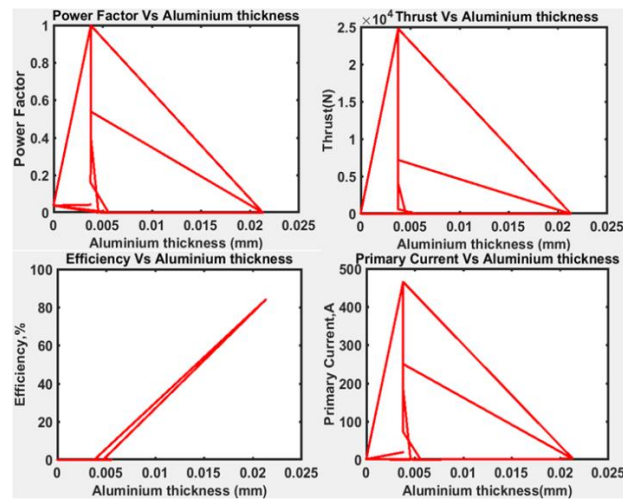


Figure 8 GA Optimization for Design Variables,  $I_{primary}$ ,  $\eta$ , PF and Thrust for aluminum thickness

Parameter	Iterative	GA	COA	GA_COA
Efficiency (%)	78.4	78.9	79.2	80.4
Power factor	0.76	0.73	0.75	0.78
Maximum thrust slip	0.5	0.5	0.5	0.5
Aluminum thickness	6	6.4	5.8	5.2
Primary width/pole pitch	0.002	0.002	0.002	0.002
Primary current density $A/m^2$	467	470	465	490

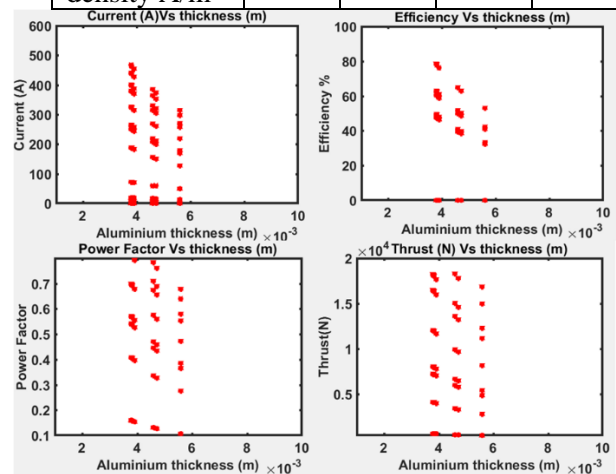


Figure 9 GA with COA Optimization for Design Variables,  $I_{primary}$ ,  $\eta$ , PF and Thrust for aluminum thickness

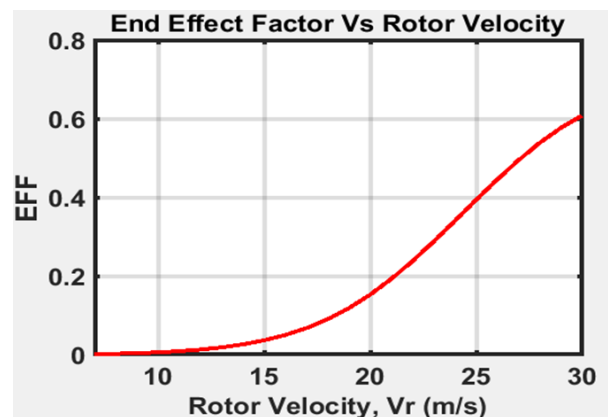


Figure 10 End effect factor (EEF) Vs rotor velocity

In table 3, the motor parameters using conventional iterative with equations, genetic algorithm (GA), Cuckoo optimization algorithm (COA) and genetic algorithm (GA) with cuckoo optimization algorithm (COA) design optimization procedures are stated. Conventional motor parameters, GA, COA and GA with COA investigate the outcomes are depicted. Table 3 reflects that GA with COA produces optimal results for motor performance, followed by GA, COA and usual iterative equations.

Figure 8 depicts the performance of motor on Thrust, efficiency, power factor and primary current for different aluminum thickness using GA optimization technique. Figure 9 depicts the performance of motor on Thrust, efficiency, power factor and primary current for different aluminum thickness using GA-COA combined optimization technique. Also, end effect factor is determined using following equation, refer Figure 10

$$EEF = \frac{P_{ag(ne)} - P_{ag(we)}}{P_{ag(ne)}} = 1 - \frac{P_{ag(we)}}{P_{ag(ne)}}$$

## CONCLUSIONS

It is too hard to find optimal parameters of motor for maximal performance using equations as it involves complicated observations. This paper used bio inspired optimization algorithms to explore for optimal design parameters. Hence it compared three different algorithm choices like GA, COA and combined GA-COA for optimally designing three-phase 440V operated SSLIM. Though every parameter is crucial in design of motors, certain motor parameters are realistically useful and very directly important for applications, they are the thrust, efficiency, power factor and primary current. Comparison of the optimal designs using GA and COA optimizations implied that the profit of the proposed performance using GA with COA is even better than anticipated. Larger efficiency, high thrust, high power factor and less primary current for SSLIM designs can be referred.

## REFERENCES

- [1] Xu W., Hu D., Mu C.X., "Novel efficiency optimization control algorithm for single-sided linear induction motor", IEEE International Conference on Applied Superconductivity and Electromagnetic Devices (2015), 48-49.
- [2] Manna M.S., Marwaha S., Marwaha A., "Eddy currents analysis of induction motor by 3D FEM" *IEEE Trans. on POWERCON-08*, 2008. pp-1-4.
- [3] Fetcher J., B. Williams and Mahmoud M., "Air gap flux fringing reduction in inductors using open circuit copper screens", IEE proceedings 2005
- [4] Gieras, J.F., "Linear Induction Drives", Oxford University Press, Inc., New York, 1994.
- [5] Pai, R.M.; Boldea, I.; Nasar, S.A. "A complete equivalent circuit of a linear induction motor with sheet secondary" *IEEE Transactions on Magnetics*, Volume: 24, Issue: 1, Jan. 1988 Pages: 639 – 654.
- [6] Nasar, S.A. and Boldea, I., "Linear Electric Motors", Prentice-Hall, Inc., Englewood Cliffs, New Jersey, 1987.
- [7] Rajabioun, R. (2011). "Cuckoo Optimization Algorithm" *Applied Soft Computing*, 11(3): 5508- 5518.
- [8] HassanpourIsfahani, A., Ebrahimi, B.M., and Lesani, H. (2008), "Design Optimization of a Low-Speed Single-Sided Linear Induction Motor for Improved Efficiency and Power Factor", *IEEE TRANSACTIONS ON MAGNETICS*, 44 (2): 23-36
- [9] N. Bianchi, S. Bolognani, "Design optimization of electric motors by genetic algorithm" *IEEE Proc Electr Power Appl.*, 145: 475-483, 1998.